Hyperfine Interact (2017) 238:66
DOI 10.1007/s10751-017-1435-5

Electrospinning synthesis and characterization of PLA-PEG-MNPs composite fibrous membranes

M. Kumar[1,2,3] · S. Klimke[1] · A. Preiss[1] · D. Unruh[1] · D. Wengerowsky[1] · R. Lehmann[1] · R. Sindelar[2] · G. Klingelhöfer[4] · R. Boča[5] · F. Renz[1,3]

Abstract An electrospinning technique was used to fabricate PLA, PLA-PEG and PLA-PEG-MNPs composite fibrous membranes. The morphology of electrospun composite membranes were characterized by scanning electron microscope. To test the potential availability of MNPs in PLA-PEG composite membranes, TG, Raman, Mössbauer, VSM and ICP-OES analysis were used. The PLA-PEG composite fibrous membranes showed the presence of MNPs, hence offers the possibility for magnetically triggered on-demand drug delivery.

Keywords Polylactic acid (PLA) · Polyethylene glycol (PEG) · Magnetic nanoparticles (MNPs) · Electrospinning · Composite fibrous membranes

This article is part of the Topical Collection on *Proceedings of the 3rd Mediterranean Conference on the Applications of the Mössbauer Effect (MECAME 2017), Jerusalem, Israel, 5–7 June 2017*
Edited by Mira Ristic, Stjepko Krehula, Israel Nowik and Israel Felner

✉ F. Renz
renz@acd.uni-hannover.de

[1] Institute of Inorganic Chemistry, Leibniz Universität Hannover, Callinstraße 9, 30167 Hannover, Germany

[2] Faculty II, University of Applied Science and Arts, Ricklinger Stadtweg 120, 30459 Hannover, Germany

[3] Hannover School for Nanotechnology, Leibniz Universität Hannover, Schneiderberg 39, 30167 Hannover, Germany

[4] Institute of Inorganic and Analytical Chemistry, Johannes Gutenberg-Universität Mainz, 55128 Mainz, Germany

[5] Institute of Inorganic Chemistry, Slovak University of Technology, 81237 Bratislava, Slovakia

Published online: 04 September 2017

1 Introduction

At present, the global advanced drug delivery market is forecast to grow at a compound annual growth rate (CAGR) of 4.9% from roughly $ 178.8 billion in 2015 to nearly $ 227.3 billion by 2020, according to recent BCC Research (Available: http://www.bccresearch.com/market-research/pharmaceuticals/advanced-drug-delivery-systems-tech-markets-report-phm006k.html). Controlled drug delivery systems are an extensively investigated research area due to its several advantages, e.g. they maintain the drug within the desired therapeutic range, preserve drugs that are rapidly dissolved in the body, therefore reducing toxicity and improving patient comfort [1]. However, in many clinical scenarios, for an effective treatment, drug delivery requires only intermittent drug administration to deal with occasional exacerbation [2]. For this reason, magnetic field based delivery systems are one of the most effective approaches for localizing drug in the living body [3], because magnetic forces can be concentrated on a local region, reducing collateral effects, and can be tolerated by the living body [4, 5]. The magnetic nanoparticles (MNPs) are used to kill the infected cells by generating heat on an alternating magnetic field [6]. It is expected that MNPs may lead to kill the healthy tissues due to overheating. Incorporation of these magnetic nanoparticles into polymer fibers could provide a solution. The MNPs incorporated polymer fibers are useful in mass transport properties, mechanical stability, and large surface areas of active reaction sites [7]. One application of such magnetic polymer fibers is the on-demand delivery of drug [8].

The drug carrier composed with MNPs and polymer composite fibrous membranes, should satisfy some conditions for biomedical applications like; (1) biodegradability, (2) no toxicity, and (3) no iron leakage [9]. Polylactic acid (PLA) fulfills some of these conditions and it is being used in biomedical applications [10]. One challenge of using PLA is its hydrophobicity [11]. Therefore, to decrease its hydrophobicity and increase its solubility Polyethylene glycol is incorporated [12]. And to gain magnetic properties, silica-coated magnetite (MagSilica®; $Fe_3O_4@SiO_2$) is embedded. Silica coating helps in dispersing magnetite in the liquid media and keep the surface functional [13].

In this paper, PLA, PLA-PEG and PLA-PEG-MNPs composite fibrous membranes were fabricated by electrospinning technique. These composite membranes were characterized by Scanning electron microscopy (SEM), Thermogravimetric analysis (TGA), Micro Raman spectroscopy (MRS), Mössbauer spectroscopy (MS), Vibrating sample magnetometer (VSM) and Inductively coupled plasma optical emission spectrometry (ICP-OES).

2 Experimental

2.1 Materials used

All chemicals were of analytical grade and used without prior treatment. Polylactic acid 6202 (PLA) was provided by Prof. Dr. –Ing. Hans-Josef Endres, Institute for Bioplastics and Biocomposites (Ifbb) Hannover, Germany. Silica-coated magnetite nanoparticles (MagSilica®; $Fe_3O_4@SiO_2$) as magnetic nanoparticles (MNPs) was purchased from Evonik formally Degussa AG, Germany. Polyethylene glycol 1500 (PEG) was purchased from abcr, Germany and trichloromethane (TCM) from Roth, Germany.

3 Material characterization

3.1 Scanning electron microscopy (SEM)

Scanning electron microscope (SEM) (Zeiss Leo VP 1455) was used to analyze the surface morphology and diameter of the prepared fibers. All specimens were coated (SC7620 Mini Sputter Coater, Quorum Technologies) with a conductive layer of platinum or gold of about 10 nm thickness before taking SEM images.

3.2 Thermogravimetric analysis (TGA)

To study thermal degradation of PLA-PEG and PLA-PEG-MNPs composite fibrous membranes, TGA (NETZSCH STA 409, Germany) was conducted under argon atmosphere. The applied heating rate was 10 K/min, and the scanning range was from 40 to 500 °C. All specimens with a weight of approximately 8–10 mg were used.

3.3 Micro Raman spectroscopy (MRS) measurements

Raman spectra were scanned on a SENTERRA Dispersive Raman Microscope Spectrometer (Bruker Optik GmbH, Germany) with a thermoelectrically cooled CCD detector (charge–coupled device). For the analysis, a diode laser with the excitation wavelength of 785 nm was used. All specimens were analyzed with an Olympus LWD 50× (NA = 0.50) microscope in a spectral range from 90 to 3500 cm^{-1} (2 s integration time, 5 accumulations, 100 mW laser power). All these samples were measured at a controlled temperature of (22 ± 1) °C.

3.4 Mössbauer spectrometer

The Mössbauer measurements were performed in transmission geometry with a MIMOS II (Space and Earth Science Instrumentation) at 298 K. All measurements were recorded with 14.4 keV. The source were ^{57}Co nuclei in Rh matrix. The environment was protected by a lead cover from gamma radiation. All isomer shifts were given relative to α-Fe.

3.5 Vibrating sample magnetometer (VSM)

To study magnetic properties (M–H curves) of the pure MNPs and PLA-PEG-MNPs composite fibrous membranes, VSM (EG&G Princeton Applied Research Model 4500) were performed. All the specimens were measured at a room temperature.

3.6 Inductively coupled plasma optical emission spectrometry (ICP-OES)

The contents of iron and silicon in the PLA-PEG-MNPs composite fibers were determined by ICP-OES measurement (Arcos FHS12, SPECTRO Analytical Instrument GmbH). For this about 150 mg of the composite fibers were dissolved in 5 ml conc. nitric acid by microwave digestion (turbo WAVE, MLS GmbH). After digestion, the solutions were filled with ultrapure water to a volume of about 15 ml, 100-fold diluted and analyzed by ICP-OES. For quantification, an external calibration model with 5 standard solutions was performed.

Table 1 Summary of electrospinning conditions

Sample	Concentration [wt %]	Flow rate [$mL\ h^{-1}$]	Voltage [kV]	Height [cm]	Rotor speed [m/s]	Mean diameter [$\mu m \pm SD$]
PLA	8	1	12	10	–	6.49 ± 1.9
PLA-PEG	8-8	1	12	12	10	2.78 ± 0.4
PLA-PEG-MNPs	8-8-3	2	12	15	10	2.0 ± 0.4

Calibration and evaluation are based on DIN 38402-51 and DIN 32645 with $k = 2$ and $P = 95\%$ for the extended measurement uncertainty.

3.7 Synthesis of PLA, PLA-PEG, and PLA-PEG-MNPs composite fibrous membranes

PLA, PLA-PEG and PLA-PEG-MNPs composites fibrous membranes were prepared by electrospinning technique. 8 wt% of PLA in trichloromethane (TCM) was dissolved by constant stirring for 10 h at 24 °C. To this, 8 wt% of PEG was added slowly and stirred for 5 h to obtain a homogeneous PLA-PEG viscous solution. 3 wt% of MNPs were dispersed with methanol and mix into composite solution of PLA-PEG. The composite solution of PLA-PEG-MNPs were stirred for another 5 h. This composite solution (PLA, PLA-PEG and PLA-PEG-MNPs) was separately packed in 10 ml syringe equipped with a $21 \times 7/8$ G conducting needle and connected to electrospinning [14]. Table 1 shows parameter used for electrospinning experiments.

4 Results and discussion

4.1 Scanning electron microscopy (SEM) analysis

SEM images of PLA, PLA-PEG and PLA-PEG-MNPs composite fibrous membranes are shown in Fig. 1. Figure 1a shows a typical porous-fiber morphology, which is mainly attributed to the rapid evaporation of the solvent (TCM) during electrospinning [15]. The mean diameter of the PLA fibrous membranes is $6.5 \pm 1.9\ \mu m$. The fibers diameter and morphology is affected when PEG copolymer is incorporated to PLA by a factor of around two [16], as seen in Fig. 1b. This happened because PEG works as a plasticizer which attributes to decrease in PLA-PEG fiber diameter [17]. The mean diameter of the PLA-PEG composite fibrous membranes is $2.8 \pm 0.4\ \mu m$. Improved fiber uniformity is observed because of the flexible PEG chains in PLA fibers. Figure 1c revealed that the PLA-PEG-MNPs composite fibers have randomly distributed beads in the form of MNPs in PLA-PEG composite membranes. The mean diameter of the PLA-PEG-MNPs fibrous membranes is $2.0 \pm 0.4\ \mu m$. Figure 1d revealed the mean fiber diameter distribution of these composite membranes.

4.2 Thermal analysis

The thermal behavior of electrospun PLA-PEG and PLA-PEG-MNPs composite fibrous membranes is investigated by TGA analysis, shown in Fig. 2. PLA-PEG composite fibrous membranes show two step weight loss (Fig. 2a). In the first interval, from 225 to 370 °C

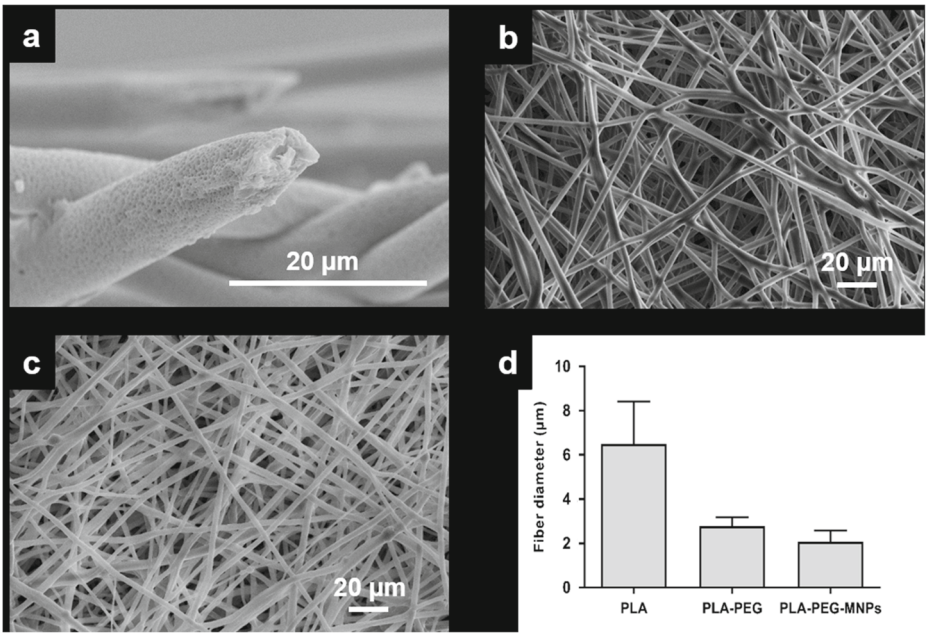

Fig. 1 Scanning electron micrographs for electrospun **a** PLA **b** PLA-PEG **c** PLA-PEG-MNPs and **d** Average mean diameter of these composite fibrous membranes

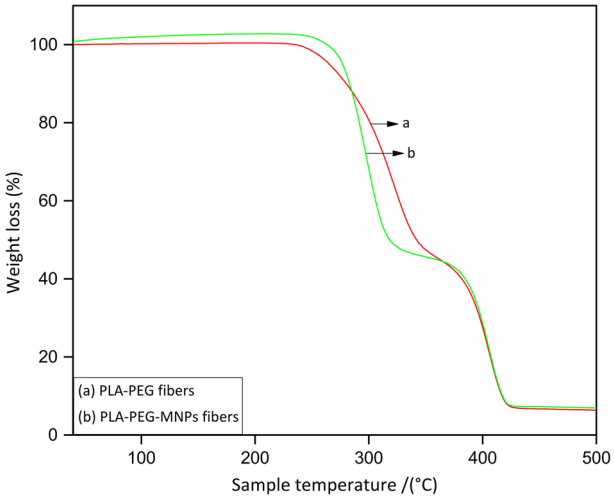

Fig. 2 Thermal degradation of **a** PLA-PEG **b** PLA-PEG-MNPs composite fibrous membranes as measured through TGA

there is 55% weight loss which is corresponding to the PLA. In the second interval, from 370 to 450 °C there is 39% weight loss which is corresponding to PEG. PLA-PEG-MNPs composite fibrous membranes also show two step weight loss (Fig. 2b). In the first interval, from 230 to 350 °C there is 57% weight loss. In the second interval, from 350 to 450 °C

Table 2 Thermogravimetric data table for PLA-PEG and PLA-PEG-MNPs composite fibrous membranes

Sample	Weight loss interval	T_{onset} °C (± 3 °C)	T_{endset} °C (+/ − 3 °C)	Weight loss
PLA-PEG	2	225	370	55.11
		370	450	38.85
PLA-PEG-MNPs	2	230	350	57.07
		350	450	38.67

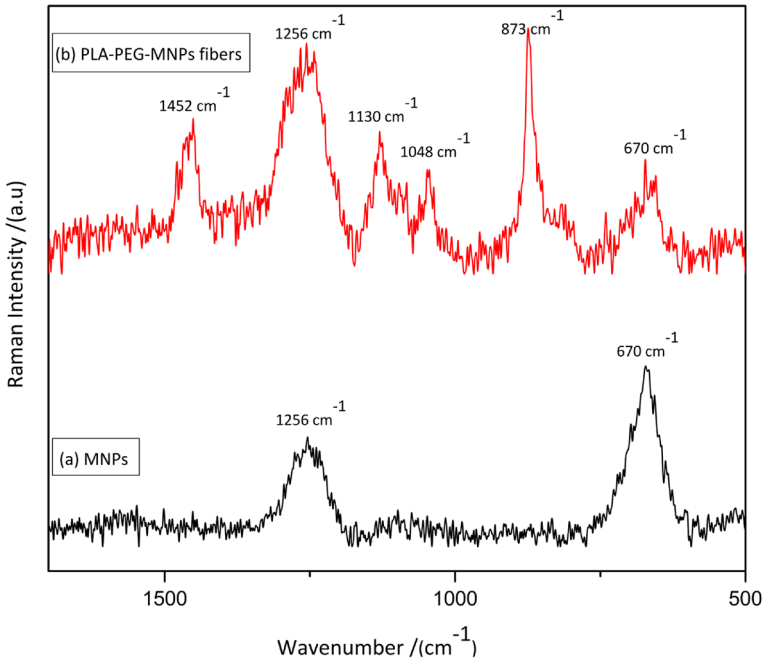

Fig. 3 Raman spectra of **a** Magnetic nanoparticles (MNPs) and **b** PLA-PEG-MNPs composite fibrous membranes

there is 39% weight loss. From TGA analysis, it is confirmed that the PLA-PEG composite membrane is modified by MNPs. Table 2 show all the treatments.

4.3 Raman analysis

The Raman spectra of MNPs and PLA-PEG-MNPs composite fibrous membranes with the main bands are shown in Fig. 3. The signals of MNPs at 670 cm^{-1} and 1256 cm^{-1} are assigned to the Si-O-Si and C=S vibration (Fig. 3a). The same bands exist in PLA-PEG-MNPs composite fibers, which clearly indicate the presence of MNPs in the polymer fibers (Fig. 3b). The band associated with CH_3 asymmetric deformation vibration is observed for PLA at about 1452 cm^{-1} [18, 19]. The C–COO stretching of the repeated unit is responsible for the very strong band at 873 cm^{-1} for PLA, as previously observed by Kister et al. [19].

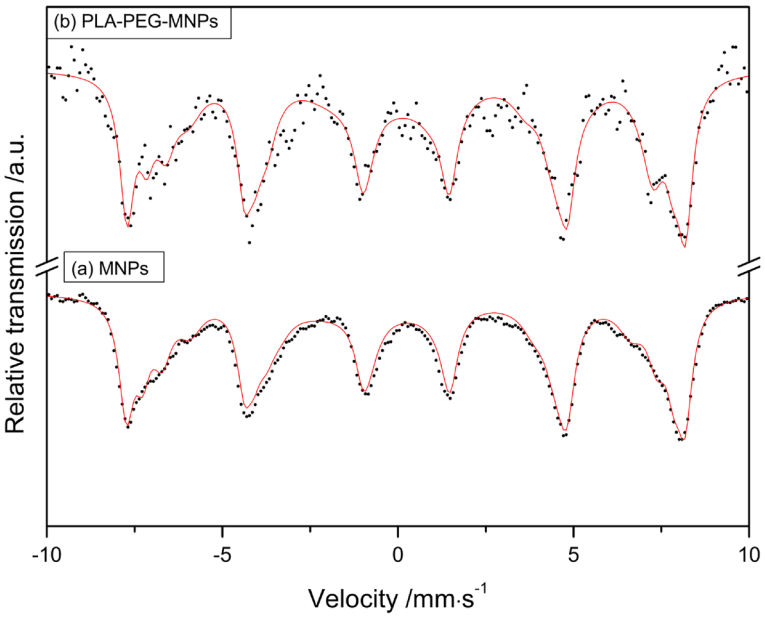

Fig. 4 Mössbauer spectra of **a** Magnetic nanoparticles (MNPs) and **b** PLA-PEG-MNPs composite fibrous membranes measured at room temperature

Two other bands appear near 1130 and 1048 cm^{-1} and are assigned to rCH_3 rocking and $C\text{-}CH_3$ stretching mode, respectively [18].

4.4 Mössbauer analysis

Mössbauer is carried out to further confirm the presence of MNPs in PLA-PEG composite fibrous membranes [20]. Figure 4 shows a typical Mössbauer spectrum of MNPs and PLA-PEG-MNPs composite fibrous membranes. A small variation in intensities of PLA-PEG-MNPs (Fig. 4b) composite fibrous membranes is observed in comparison to the pure MNPs (Fig. 4a). This could be caused due to the size distribution of the MNPs in PLA-PEG composite membranes [21]. A small changes in the values of the magnetic hyperfine splitting indicate that the magnetic properties of the nanoparticles could be preserved. The distributed sextets are assigned to the small size of the particles, thermal agitation and impurities of the sample [22]. For the fit, four sextets are used to describe the magnetic hyperfine splitting. The effective magnetic fields of sextet 1 ($B_{hf} = 49.32(7)$) and 2 ($B_{hf} = 46.90(13)$) are characteristic for magnetite whereby the first can be associated with the iron in site A and sextet two to the iron in site B of the spinal structure [13]. Table 3 shows parameters of Mössbauer spectra at 298 K for MNPs and PLA-PEG-MNPs composite fibrous membranes.

4.5 VSM analysis

The magnetic characteristics of the MNPs and PLA-PEG-MNPs composite fibrous membranes are investigated by a vibration sample magnetometer (VSM), shown in Fig. 5. Based on results, the saturation magnetization (M_s), remnant magnetization (M_r) and coercive

Table 3 Parameters of the Mössbauer spectra of silica-coated magnetic nanoparticles (MNPs) and PLA-PEG-MNPs composite fibrous membranes

Sample	Component	δ (mm/s)	ε_Q (mm/s)	B_{hf} (T)	Δw (mm/s)	Population (%)
MNPs	Sextet 1	0.34(1)	−0.01	49.32(7)	0.26(1)	38.50(31)
	Sextet 2	0.39(1)	0.01(1)	46.90(13)	0.26(4)	20.80(49)
	Distr. Sextet 1	0.43(2)	0.00(2)	43.69(16)	0.33(4)	23.50(47)
	Distr. Sextet 2	0.41(3)	0.05(3)	38.88(29)	0.43(6)	17.20(33)
PLA-PEG-MNPs	Sextet 1	0.34(3)	0.01(3)	49.26(23)	0.26(3)	38.40(49)
	Sextet 2	0.43(7)	0.06(7)	46.26(51)	0.26(7)	19.10(57)
	Distr. Sextet 1	0.43(8)	0.00(8)	42.97(63)	0.37(9)	23.50(71)
	Distr. Sextet 2	0.32(18)	0.42(17)	40.70(13)	0.55(23)	19.00(82)

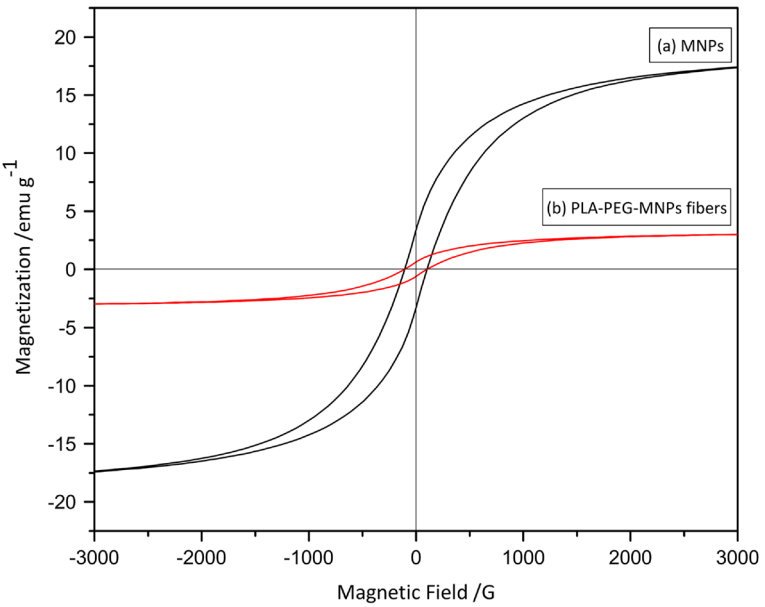

Fig. 5 Magnetization curves for **a** Magnetic nanoparticles (MNPs) and **b** PLA-PEG-MNPs composite fibrous membranes measured at room temperature

field (H_c) of pure MNPs are found to be 16.46 emu g^{-1}, 3.76 emu g^{-1} and 108.7 G, respectively; however, the PLA-PEG-MNPs composite fibrous membranes adequate considerably lower M_s, M_r and H_c value 2.84 emu g^{-1}, 0.72 emu g^{-1} and 105. 6 G, respectively [23]. This results suggest that PLA-PEG-MNPs composite fibrous membranes retained magnetic properties [14].

4.6 Inductively coupled plasma optical emission spectrometry (ICP-OES) analysis

ICP-OES analysis is well suited for an accurate determination of elemental compositions of various samples. Therefore, the contents of Fe and Si inside PLA-PEG-MNPs composite

fibrous membranes are analyzed after acid digestion. PLA-PEG-MNPs composite fibers show an iron content of 3.50 ± 0.08 wt.% and silicon content of 1.29 ± 0.10 wt.%. These results show the exact metal content of MNPs in the PLA-PEG composite fibrous membranes.

5 Conclusion

In conclusion, we have presented a simple and effective technique, electrospinning, for fabricating PLA, PLA-PEG and PLA-PEG-MNPs composite fibrous membranes. SEM analysis showed that the fibers are porous and cylindrical. The mean diameter decreases with blending PEG and MNPs to PLA while the fiber morphology remains constant. Thermal, Raman, Mössbauer and VSM analysis shows the presence of MNPs in PLA-PEG composite membranes. ICP-OES analysis confirmed the contents of Fe and Si in PLA-PEG-MNPs composite membranes. The results are promising for further investigation of on-demand drug delivery.

Acknowledgements The authors gratefully acknowledge Hannover School for Nanotechnology, Germany for their financial supports. We would like to thank M.Sc. Fabian Zimmermann, Institut für Analytical Chemistry, LUH, Hannover for access and assistance to Raman and ICP-OES analysis and Dr.-Ing. Marc Christopher Wurz, Institut für Mikroproduktionstechnik, LUH, Hannover for VSM.

References

1. Zeng, J., et al.: Biodegradable electrospun fibers for drug delivery. J. Control. Release **92**(3), 227–231 (2003)
2. Edelman, E.R., Langer, R.: Optimization of release from magnetically controlled polymeric drug release devices. Biomaterials **14**(8), 621–626 (1993)
3. Andrä, W., Nowak, H.: Magnetism in Medicine. Wiley-VCH Verlag GmbH & Co KGaA, Weinheim (2007)
4. Yellen, B.B., et al.: Targeted drug delivery to magnetic implants for therapeutic applications. J. Magn. Magn. Mater. **293**(1), 647–654 (2005)
5. Iannone, A., et al.: Blood clearance of dextran magnetite particles determined by a noninvasive in vivo ESR method. Magn. Reson. Med. **22**(2), 435–442 (1991)
6. Hilger, I., Frühauf, K., Andrä, W., Hiergeist, R., Hergt, R., Kaiser, W.A.: Heating potential of iron oxides for therapeutic purposes in interventional radiology. Acad. Radiol. **9**(2), 198–202 (2002)
7. Thévenot, J., Oliveira, H., Sandre, O., Lecommandoux, S.: Magnetic responsive polymer composite materials. Chem. Soc. Rev. **42**(17), 7099 (2013)
8. Fernandez-Pacheco, R., et al.: Magnetic nanoparticles for local drug delivery using magnetic implants. J. Magn. Magn. Mater. **311**(1 Spec. Iss.), 318–322 (2007)
9. Landfester, K., Ram rez, L.P.: Encapsulated magnetite particles for biomedical application. J. Phys. Condens. Matter **15**(15), S1345–S1361 (2003)
10. Lasprilla, A.J.R., Martinez, G.A.R., Lunelli, B.H., Jardini, A.L., Filho, R.M.: Poly-lactic acid synthesis for application in biomedical devices—a review. Biotechnol. Adv. **30**(1), 321–328 (2012)
11. Chaiwong, C., Rachtanapun, P., Wongchaiya, P., Auras, R., Boonyawan, D.: Effect of plasma treatment on hydrophobicity and barrier property of polylactic acid. Surf. Coatings Technol. **204**(18–19), 2933–2939 (2010)
12. Sheth, M., Kumar, R.A., Dave, V., Gross, A.R., McCarthy, P.S.: Biodegradable polymer blends of poly (lactic acid) and poly (ethylene glycol). J. Appl. Polym. Sci. **66**, 1495–1505 (1996)
13. Ferreira, R.V., et al.: Synthesis and characterization of silica-coated nanoparticles of magnetite. Hyperfine Interact. **195**(1), 265–274 (2009)
14. Kumar, M., Unruh, D., Sindelar, R., Renz, F.: Preparation of magnetic polylactic acid fiber mats by electrospinning. Nano Hybrids Compos. **14**, 39–47 (2017)
15. Bognitzki, M., et al.: Nanostructured fibers via electrospinning. Adv. Mater. **13**, 70–72 (2001)

16. Toncheva, A., et al.: Antibacterial PLA/PEG electrospun fibers: comparative study between grafting and blending PEG. Eur. Polym. J. **75**, 223–233 (2016)
17. Kumar, M., et al.: Mixture of PLA-PEG and biotinylated albumin enables immobilization of avidins on electrospun fibers. J. Biomed. Mater. Res. - Part A **105A**, 356–362 (2017)
18. Kister, G., Cassanas, G., Vert, M., Pauvert, B., Tébol, A.: Vibrational analysis of poly(L-lactic acid). J. RAMAN Spectrosc. **26**, 307–311 (1995)
19. Kister, G., Cassanas, G., Vert, M.: Effects of morphology, conformation and configuration on the IR and Raman spectra of various poly(lactic acid)s. Polymer (Guildf). **39**(2), 267–273 (1998)
20. Meyer, T., et al.: Electrospun complexes—functionalised nanofibres. Hyperfine Interact. **237**(1), 1–11 (2016)
21. Pan, W., Han, R., Chi, X., Liu, Q., Wang, J.: Ferromagnetic Fe3O4 nanofibers: electrospinning synthesis and characterization. J. Alloys Compd. **577**(3), 192–194 (2013)
22. Mahmed, N., Heczko, O., Lancok, A., Hannula, S.P.: The magnetic and oxidation behavior of bare and silica-coated iron oxide nanoparticles synthesized by reverse co-precipitation of ferrous ion (Fe 2+) in ambient atmosphere. J. Magn. Magn. Mater. **353**, 15–22 (2014)
23. Cullity, B.D., Graham, C.D.: Introduction to Magnetic Materials. Wiley, New York (2009)